Chem

CellPress

Article

Reversible Nitrogen Fixation Based on a Rechargeable Lithium-Nitrogen Battery for Energy Storage

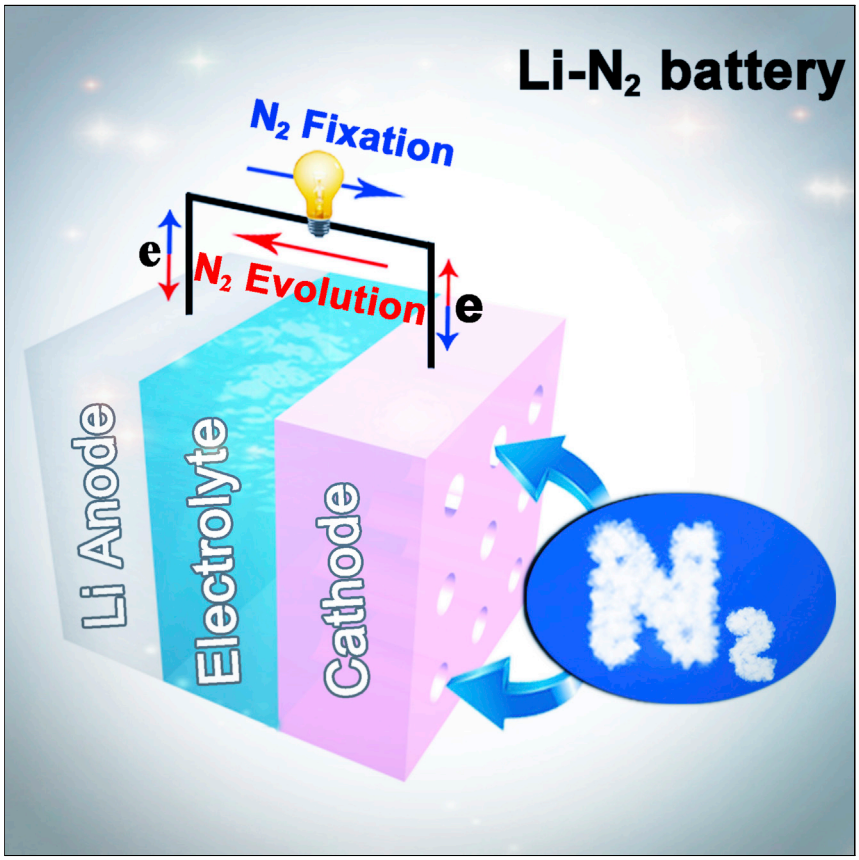

Based on a rechargeable lithium-nitrogen battery, an advanced strategy for reversible nitrogen fixation and energy conversion has been successfully implemented at room temperature and atmospheric pressure. It shows a promising nitrogen fixation faradic efficiency and superior cyclability.

Jin-Ling Ma, Di Bao, Miao-Miao Shi, Jun-Min Yan, Xin-Bo Zhang

xbzhang@ciac.ac.cn

HIGHLIGHTS

A rechargeable Li-N_2 battery is proposed for a reversible N_2 fixation process

The Li-N_2 battery provides technological progress in N_2 fixation

The Li-N_2 battery shows high faradic efficiency for N_2 fixation

The catalyst can improve faradic efficiency and decrease energy consumption

Ma et al., Chem 2, 525–532
April 13, 2017 © 2017 Elsevier Inc.
http://dx.doi.org/10.1016/j.chempr.2017.03.016

Chem

CellPress

Article

Reversible Nitrogen Fixation Based on a Rechargeable Lithium-Nitrogen Battery for Energy Storage

Jin-Ling Ma,[1,2,4] Di Bao,[1,4] Miao-Miao Shi,[1,3] Jun-Min Yan,[3] and Xin-Bo Zhang[1,5,*]

SUMMARY

Although the availability of nitrogen (N_2) from the atmosphere for N_2 fixation is limitless, it is immensely challenging to artificially fix N_2 at ambient temperature and pressure given the element's chemical inertness and stability. In this article, as a proof-of-concept experiment, we report on the successful implementation of a reversible N_2 cycle based on a rechargeable lithium-nitrogen (Li-N_2) battery with the proposed reversible reaction of $6Li + N_2 \leftrightharpoons 2Li_3N$. The assembled N_2 fixation battery system, consisting of a Li anode, ether-based electrolyte, and a carbon cloth cathode, shows a promising electrochemical faradic efficiency (59%). The unique properties of Li-N_2 rechargeable batteries not only provide promising candidates for N_2 fixation but also enable an advanced N_2/Li_3N cycle strategy for next-generation electrochemical energy-storage systems.

INTRODUCTION

The conversion of atmospheric nitrogen (N_2) into valuable substances such as fine chemicals and fertilizers is critical to industry, agriculture and many other processes that sustain human life. Although it constitutes about 78% of Earth's atmosphere, N_2 in its molecular form is unusable in most organisms because of its strong nonpolar N≡N covalent triple-bond energy, negative electron affinity, high ionization energy, and so on.[1–3] In terms of energy efficiency, the honorable Haber-Bosch process, which was put forward more than 100 years ago, is the most efficient process for producing the needed N_2 fertilizers from atmospheric N_2 in industrial processes. However, the energy-intensive Haber-Bosch process is inevitably associated with major environmental concerns under high temperature and pressure, leaving almost no room for further improvement by industry optimization, as indicated in Figure S1.[4,5] For the development of a more environmentally benign process, a variety of processes have been studied over the past few years, including non-thermal and thermal plasma fixation synthesis, biomimetic processes, and metal-complex catalysis methods. Despite the significant achievements that have been made, they still face some challenges, such as complex and expensive catalysts and electrolytes, irreversible reactions, and low yields under mild conditions.[6–13]

Inspired by rechargeable metal-gas batteries such as Li-O_2,[14–17] Li-CO_2,[18] Li-SO_2,[19] Al-CO_2,[20] and Na-CO_2[21] (which have attracted much attention because of their high specific energy density and ability to reduce gas constituent), research on Li-N_2 batteries has not seen any major breakthroughs yet. Although Li-N_2 batteries have never been demonstrated in rechargeable conditions, the chemical process is similar to that of the previously mentioned Li-gas systems. During discharging reactions, the injected N_2 molecules accept electrons from the cathode surface, and the

The Bigger Picture

The conversion of atmospheric nitrogen (N_2) into valuable substances such as fine chemicals and fertilizers is critical to industry, agriculture, and many other processes that sustain human life. However, because the N≡N bond in N_2 is one of the strongest available, N_2 fixation is a kinetically complex and energetically challenging reaction. Up until now, it has heavily relied on the energy- and capital-intensive Haber-Bosch process, wherein the input of H_2 and energy is largely derived from fossil fuels, thus resulting in large amounts of CO_2 emission. Electrocatalytic N_2 fixation represents an attractive prospect. Unfortunately, given the lack of an efficient process, the production yields and faradic efficiency are still rather poor. In this work, we propose and demonstrate a rechargeable Li-N_2 battery with the reversible reaction of $6Li + N_2 \leftrightharpoons 2Li_3N$. The battery shows a promising electrochemical faradic efficiency (59%) and good cycle performance.

activated N_2 molecules subsequently combine with Li ions to form Li-containing solid discharge products. From the results of theoretical calculations, the proposed Li-N_2 batteries show an energy density of 1,248 Wh kg^{-1}, which is comparable to that of rechargeable Li-SO_2 and Li-CO_2 batteries, as summarized in Table S1. Most importantly, N_2 fixation via Li-N_2 batteries has many environmental advantages, given that it requires only electricity and N_2 as feedstock under mild conditions. This means that without the need for large-scale, high-temperature, and high-pressure ammonia synthesis plants, rechargeable Li-N_2 batteries could be used flexibly and produce fine chemicals or N_2 where they are needed.

Herein, as a proof-of-concept experiment, we propose and demonstrate that a rechargeable Li-N_2 battery is possible under room temperature and atmospheric pressure with the following reversible battery reactions:

$$\text{anode: } 6Li \leftrightharpoons 6Li^+ + 6e^- \quad \text{(Equation 1)}$$

$$\text{cathode: } 6Li^+ + N_2 + 6e^- \leftrightharpoons 2Li_3N \quad \text{(Equation 2)}$$

$$\text{overall: } 6Li^+ + N_2 \leftrightharpoons 2Li_3N \quad \text{(Equation 3)}$$

The proposed Li-N_2 battery, which contains a Li-foil anode, glass fiber separator, ether-based electrolyte, and a carbon cloth (CC) cathode (as shown in Figures 1A and S2), holds a N_2 fixation faradic efficiency (FE) of up to 59%. Because catalysts can be critical factors for improving the N_2 fixation efficiency, Ru-CC and ZrO_2-CC composite cathodes were also investigated in this study. Impressively, the assembled Li-N_2 batteries with catalyst showed higher FE than pristine CC cathodes. Given the above, this promising research on highly efficient Li-N_2 batteries not only provides fundamental and technological progress in energy-storage systems but also enables an advanced N_2/Li_3N cycle for a reversible N_2 fixation process.

RESULTS AND DISCUSSION

In this work, both the applied current density (mA cm^{-2}) and achieved specific capacity (mAh cm^{-2}) were normalized to the area of the cathodes. In the rechargeable Li-N_2 battery, Li^+ combines with N_2 to form Li_3N during discharge, which is decomposed into Li and N_2 upon the charging process, corresponding to the above Equation 3. The electrolyte is 1 M $LiCF_3SO_3$ in tetraethylene glycol dimethyl ether (TEGDME) in consideration of its low volatility,[22,23] relative stability to Li metal and Li_3N (Figure S3), and high ionic conductivity. The CC cathode depicts a porous cross-linking structure with a geometric area of 2.0 cm^2 (Figure S4) and acts as both as a conductive network and reaction site for nucleating and anchoring discharge products. Its porous structure is able to store large amounts of N_2 fixation products without blocking air channels and benefits the cathode reaction in the gas-electrolyte-cathode material interface. As depicted in Figure 1A, once the anode and cathode are connected externally, the Li-N_2 battery with reaction $6Li + N_2 = 2Li_3N$ supplies electric energy upon discharge and recovery upon charge.

Figure S5 shows the galvanostatic discharging curves of the assembled battery in Ar- and N_2-saturated atmospheres, and the electrochemical reaction in the Ar atmosphere is similar to $Li \rightarrow Li^+$ with an intercalation reaction.[24] The X-ray diffraction (XRD) pattern of products on the CC electrode in Ar showed a negative shift for the (002) crystal face of graphite,[24] further indicating the occurrence of an

[1]State Key Laboratory of Rare Earth Resource Utilization, Changchun Institute of Applied Chemistry, Chinese Academy of Sciences, Changchun 130022, Jilin, China

[2]University of Chinese Academy of Sciences, Beijing 100049, China

[3]Key Laboratory of Automobile Materials, Ministry of Education and College of Materials Science and Engineering, Jilin University, Changchun 130012, Jilin, China

[4]These authors contributed equally

[5]Lead Contact

*Correspondence: xbzhang@ciac.ac.cn

http://dx.doi.org/10.1016/j.chempr.2017.03.016

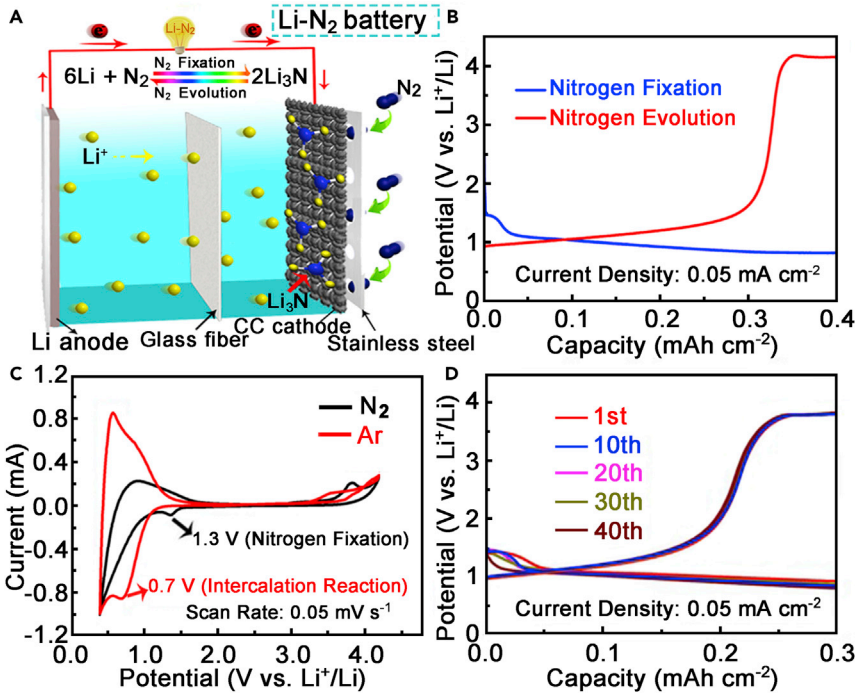

Figure 1. The Structure and Rechargeability of a Room-Temperature Li-N_2 Battery

(A) Structure of a Li-N_2 battery with a Li-foil anode, ether-based electrolyte, and CC cathode.

(B) N_2 fixation (blue) and N_2 evolution (red) curves of a Li-N_2 battery with a CC cathode at a current density of 0.05 mA cm^{-2}.

(C) CV curves of a Li-N_2 battery at a scan rate of 0.05 mV s^{-1} in N_2-saturated (black) and Ar-saturated (red) atmospheres.

(D) Cyclic performance of a Li-N_2 battery at a current density of 0.05 mA cm^{-2}.

intercalation reaction (Figure S6). In contrast, the discharging curve in the N_2 atmosphere showed a plateau from 1.2 to ~0.8 V, which might indicate a multi-step reaction of N_2 adsorption and/or multiple electron-transfer processes.[25] Figure 1B displays a typical charge-discharge curve of the Li-N_2 battery at atmospheric pressure and room temperature. The high charge overpotential at the end of the charge might be due to some side reactions, such as electrolyte and/or cathode decomposition. In addition, cyclic voltammetry (CV) was measured from 0.4 to 4.2 V for further examination of the N_2 fixation and evolution reaction on the CC cathode between the N_2 and Ar atmospheres (Figure 1C). Obviously, different cathodic peaks were observed in the CV curves under different atmospheres, and the cathodic peak at 1.3 V in the N_2 atmosphere (black curve) could be assigned to the electrochemical N_2 fixation reaction. Correspondingly, the cathodic peak at 0.7 V in the Ar atmosphere (red curve) could be due to the formation of intercalation compound. Furthermore, cycling performance tests in Figure 1D were subjected to a current density of 0.05 mA cm^{-2} and a limited capacity of 0.30 mAh cm^{-2}. The results demonstrated that discharge and charge potentials underwent slight deviations even in the initial 40 cycles. This limited cycle life of the Li-N_2 battery possibly resulted from the instability of the anode and cathode, which was verified by scanning electron microscopy (SEM) of the cycled Li anode and by X-ray photoelectron spectroscopy (XPS) of the cycled CC cathode; the Li anode surface turned from smooth to rough, and the O content of the cycled CC cathode increased in relation to that of the pristine one (Figures S7 and S8). Therefore, improving Li-N_2 batteries will require development of a stable anode, cathode, and electrolyte to avoid side reactions.

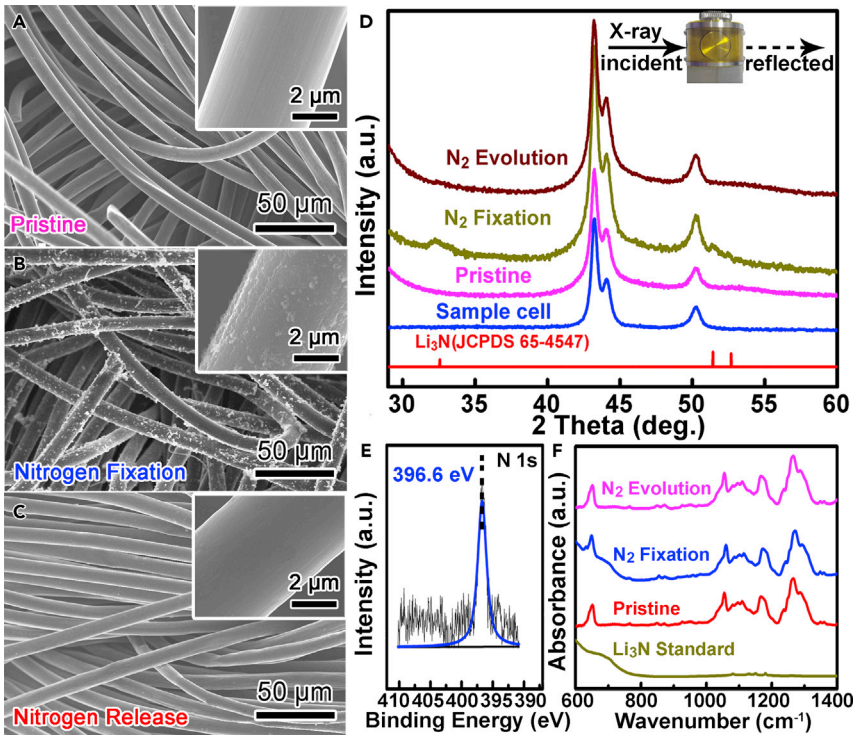

Figure 2. Ex Situ Analysis of the Electrochemical Nitrogen Fixation and Evolution Processes
SEM images (A–C), XRD patterns (D), N1s XPS spectrum (discharged CC cathode, E), and FT-IR spectra (F) of the CC cathode at different electrochemical conditions.

Furthermore, various ex situ measurements were designed to record the Li-N_2 battery reaction processes. The SEM results demonstrated that after N_2 fixation, some particles had deposited and accumulated on the CC cathode but not the pristine CC cathode (Figures 2A and 2B). Subsequently, these particles had almost disappeared, and the CC cathode recovered to a smooth surface as charging proceeded (Figure 2C). XRD, XPS, and Fourier transform infrared spectroscopy (FT-IR) were then employed to determine the composition of the above products. As shown in Figure 2D, after discharge (dark-yellow curve), besides the peaks originating from the CC substrate and the vacuum sample cell, a characteristic diffraction peak of Li_3N (JCPDS 65-4547) was observed at $2\theta = 32.4°$, consistent with the XPS result (N1s binding energy at 396.6 eV; Figure 2E).[26,27] It should be noted that we cannot exclude the formation of other Li-N compounds, such as lithium azide (LiN_3), during N_2 fixation reactions. After charging, the Li_3N characteristic peak had almost disappeared with N_2 evolution (dark-red curve), demonstrating the decomposition of Li_3N and consistent with the above SEM results. In addition, the energy-dispersive X-ray spectrometry elemental mappings in Figure S9 revealed the uniform distribution of N (28.21 atom %) on the discharged cathode; the N content was also reduced to 4 atom % after charging, indicating the decomposition of N_2 fixation products and consistent with the FT-IR results (Figure 2F).[28,29]

The concentration of Li_3N in N_2 fixation and N_2 evolution reactions was monitored with a UV-vis spectrometer by colorimetry.[30] It is known that Li_3N reacts with water immediately to form NH_3 as follows:

$$Li_3N + 3H_2O = NH_3 + 3LiOH \qquad \text{(Equation 4)}$$

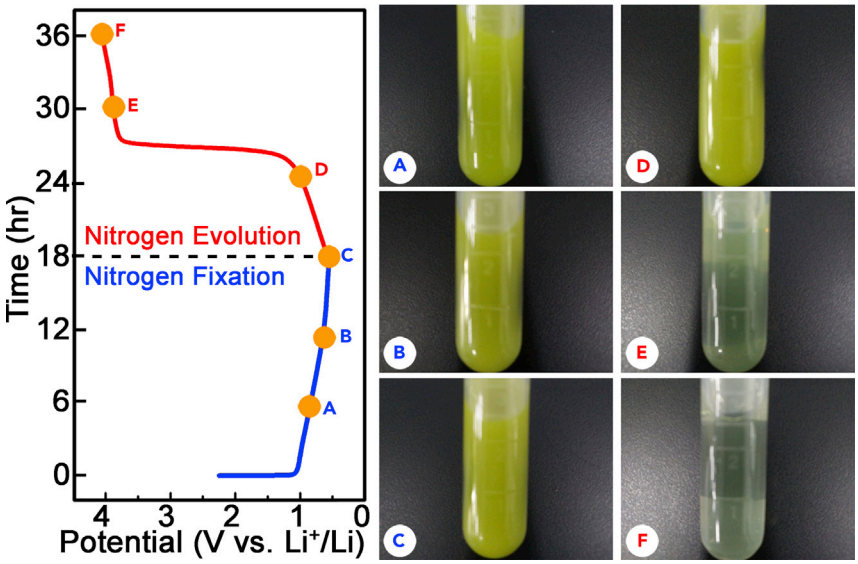

Figure 3. Colorimetric Analysis of the Electrochemical Nitrogen Fixation and Evolution Processes
The N_2 fixation (blue, A–C) and N_2 evolution (red, D–F) points were examined with Nessler's reagent via hydrolysis of Li_3N ($Li_3N + H_2O \rightarrow NH_3 + LiOH$).

The produced NH_3 derived from hydrolysis can combine with Nessler's reagent to form NH_2Hg_2OI yellow complex,

$$2[HgI_4]^{2-} + NH_3 + 3OH^- = NH_2Hg_2OI + 7I^- + 2H_2O, \qquad \text{(Equation 5)}$$

and the NH_2Hg_2OI complex presents a light absorption at 425 nm.[3] In our case, the cathodes at different charge-discharge states were immersed into the solution containing Nessler's reagent. As shown in Figure 3, the color of the solution gradually darkened from (A) to (C) as discharge time increased, demonstrating gradual accumulation of Li_3N. Variation in Li_3N during charging was also recorded at the same time intervals (Figures 3D–3F). The color gradually returned to transparent as the visible CC cathode appeared in the vessel, whereas the cathode that had not undergone an electrochemical process was transparent (Figure S10), further proving the decomposition of Li_3N upon charging. Even though the Li-N_2 cell with the CC cathode discharged in Ar, the discharged CC cathode was still transparent under colorimetric assay, and this indicated that the other compounds produced in Ar had no response to LiN_3 under colorimetric assay (Figure S11).

When considering a Li-N_2 battery as a novel electrochemical N_2 reduction method, it is necessary to determine how many N_2 fixation products are formed and the corresponding FE during N_2 fixation. As shown in Figure S12, a standard curve of NH_4^+ under low concentration was plotted according to Lambert-Beer's law, the concentration of N_2 fixation product was tested according to the standard curve, and N_2 fixation FE was acquired as follows:

$$FE = \frac{3F \times m_{NH_3-N}}{14 \times Q}, \qquad \text{(Equation 6)}$$

where 3 is the electron-transfer number of one N atom, F is the Faraday constant, m_{NH_3-N} is the measured mass of N as determined by UV-vis spectrophotometry, 14 is the molar mass of the N atom, and Q is the sum of electric charge recorded by electrochemical workstation. The results in Figure 4A demonstrate that the N_2

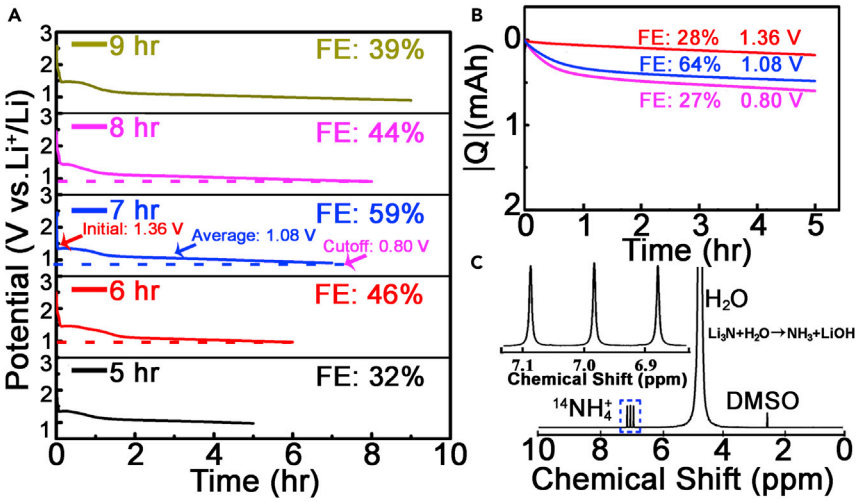

Figure 4. Faradic Efficiency of Li-N_2 Battery

(A) Galvanostatic curves and corresponding faradic efficiency (FE) at each given N_2 fixation period from 5 to 9 hr at a current density of 0.05 mA cm^{-2}.

(B) Potentiostatic curves and corresponding FE at each given N_2 fixation potential.

(C) ^{1}H NMR spectrum.

fixation FE rapidly increased from 32% (5 hr) to the maximum value of 59% (7 hr). Afterward, it reduced to 44% (8 hr) and 39% (9 hr). We also determined the FE in charge for 7 hr N_2 fixation, and the result demonstrated 87% Li_3N decomposition, corresponding to 51% FE for charging (Figure S13).

To consider the optimal potential for electrochemical N_2 fixation, we performed potentiostatic measurements at initial potential (1.36 V), average potential (1.08 V), and cutoff potential (0.80 V) according to the best FE curve (Figure 4B). After 5 hr of measurement, FE was up to 64% at 1.08 V, nearly 2.5 times higher than the other two potentials. Under the maximum yield of N_2 fixation, we further characterized N_2 fixation products by hydrolyzing to form NH_3. The obtained NH_3 protonated to NH_4^+ in the slightly acidic reaction environment (pH = 4), which was characterized by ^{1}H nuclear magnetic resonance (^{1}H NMR) (Figure 4C). The result showed that coupling of N was a triplet in DMSO-d6, as previously reported,[31] providing indirect evidence that the detected ammonia originated from the N_2 fixation product.

Because catalysts can be critical factors for electrochemical N_2 fixation, a series of catalysts, such as Ru and ZrO_2, have been studied for improved efficiency of artificial N_2 fixation process.[32,33] Therefore, we also introduced Ru-CC and ZrO_2-CC composite cathodes, prepared via high-temperature pyrolysis under H_2/Ar atmosphere, into the Li-N_2 battery (Figures S14 and S15). CV results showed that the Li-N_2 battery with the Ru-CC cathode achieved more positive cathodic potential and larger current density than that with the ZrO_2-CC or pure CC cathode (Figure S16). The galvanostatic charge-discharge measurements of the Li-N_2 batteries with different catalysts showed lower overpotential upon N_2 evolution in the N_2 atmosphere (Figure S17). The Li-N_2 batteries achieved a longer cycle life with the Ru-CC (72 cycles) or ZrO_2-CC (80 cycles) cathode than with the pure CC cathode (65 cycles) under the same test conditions, demonstrating the efficiency of catalysts in improving the stability of the cell (Figure S18). The Ru-CC and ZrO_2-CC cathodes were further subjected to potentiostatic tests at 1.08 V for 5 hr in Li-N_2 batteries. As shown in

Figure S19, the FE of the Ru-CC cathode was only 67%, lower than that of the ZrO_2-CC cathode (71%).

In conclusion, to tackle the challenges of artificial N_2 fixation under mild conditions, as a proof-of-concept experiment, we have demonstrated that electrochemical N_2 fixation in ambient conditions is possible with rechargeable Li-N_2 batteries. The electrochemical formation of Li_3N, the major N_2 fixation product of a Li-N_2 battery, was reversible in charge-discharge processes. More importantly, these results show that rechargeable Li-N_2 batteries offer a promising green candidate for N_2 fixation and enable an advanced N_2/Li_3N cycle approach for next-generation energy-storage systems. However, it should be noted that intense efforts should be devoted to developing stable anodes, cathodes, and electrolytes and investigating the underlying complex reaction mechanism of Li-N_2 batteries.

EXPERIMENTAL PROCEDURES

Full experimental procedures are provided in the Supplemental Information.

SUPPLEMENTAL INFORMATION

Supplemental Information includes Supplemental Experimental Procedures, 19 figures, and 1 table and can be found with this article online at http://dx.doi.org/10.1016/j.chempr.2017.03.016.

AUTHOR CONTRIBUTIONS

X.-B.Z. conceived the project. J.-L.M. and M.-M.S. conducted the synthesis and some physical characterizations. J.-L.M. and D.B. did the measurements and analysis and contributed equally to this work. All authors participated in writing the manuscript.

ACKNOWLEDGMENTS

This work was financially supported by the Ministry of Science and Technology of China (grants 2016YFB0100100 and 2014CB932300) and the National Natural Science Foundation of China (grants 21422108, 51472232, 51372007, and 21301014).

Received: February 6, 2017
Revised: March 16, 2017
Accepted: March 24, 2017
Published: April 13, 2017

REFERENCES AND NOTES

1. Honkala, K., Hellman, A., Remediakis, I.N., Logadottir, A., Carlsson, A., Dahl, S., Christensen, C.H., and Nørskov, J.K. (2005). Ammonia synthesis from first-principles calculations. Science *307*, 555–558.

2. Atkins, P.W., and Paula, J.D. (2002). Physical Chemistry, Seventh Edition (Oxford University Press).

3. Li, H., Shang, J., Ai, Z., and Zhang, L. (2015). Efficient visible light nitrogen fixation with BiOBr nanosheets of oxygen vacancies on the exposed {001} facets. J. Am. Chem. Soc. *137*, 6393–6399.

4. Service, R.F. (2014). Chemistry. New recipe produces ammonia from air, water, and sunlight. Science *345*, 610.

5. van Kessel, M.A.H.J., Speth, D.R., Albertsen, M., Nielsen, P.H., Op den Camp, H.J.M., Kartal, B., Jetten, M.S.M., and Lücker, S. (2015). Complete nitrification by a single microorganism. Nature *528*, 555–559.

6. Van Durme, J., Dewulf, J., Leys, C., and Van Langenhove, H. (2008). Combining non-thermal plasma with heterogeneous catalysis in waste gas treatment: a review. Appl. Catal. B *78*, 324–333.

7. Chirik, P.J. (2009). Nitrogen fixation: one electron at a time. Nat. Chem. *1*, 520–522.

8. van der Ham, C.J.M., Koper, M.T.M., and Hetterscheid, D.G.H. (2014). Challenges in reduction of dinitrogen by proton and electron transfer. Chem. Soc. Rev. *43*, 5183–5191.

9. Smil, V. (2004). Enriching the Earth: Fritz Haber, Carl Bosch, and the Transformation of World Food Production (MIT Press).

10. Kyriakou, V., Garagounis, I., Vasileiou, E., Vourros, A., and Stoukides, M. (2017). Progress in the electrochemical synthesis of ammonia. Catal. Today *286*, 2–13.

11. Montoya, J.H., Tsai, C., Vojvodic, A., and Nørskov, J.K. (2015). The challenge of electrochemical ammonia synthesis: a new perspective on the role of nitrogen scaling relations. ChemSusChem *8*, 2180–2186.

12. Marnellos, G., and Stoukides, M. (1998). Ammonia synthesis at atmospheric pressure. Science *282*, 98–100.

13. Rusanov, V.D., Fridman, A.A., and Sholin, G.V. (1981). The physics of a chemically active plasma with nonequilibrium vibrational excitation of molecules. Sov. Phys. Usp. *24*, 447–474.

14. Bruce, P.G., Freunberger, S.A., Hardwick, L.J., and Tarascon, J.M. (2011). Li-O_2 and Li-S batteries with high energy storage. Nat. Mater. *11*, 19–29.

15. Liu, T., Leskes, M., Yu, W., Moore, A.J., Zhou, L., Bayley, P.M., Kim, G., and Grey, C.P. (2015). Cycling Li-O_2 batteries via LiOH formation and decomposition. Science *350*, 530–533.

16. Lu, J., Lee, Y.J., Luo, X., Lau, K.C., Asadi, M., Wang, H.H., Brombosz, S., Wen, J., Zhai, D., Chen, Z., et al. (2016). A lithium-oxygen battery based on lithium superoxide. Nature *529*, 377–382.

17. Xu, J.J., Wang, Z.L., Xu, D., Zhang, L.L., and Zhang, X.B. (2013). Tailoring deposition and morphology of discharge products towards high-rate and long-life lithium-oxygen batteries. Nat. Commun. *4*, 2438.

18. Zhang, Z., Zhang, Q., Chen, Y., Bao, J., Zhou, X., Xie, Z., Wei, J., and Zhou, Z. (2015). The first introduction of graphene to rechargeable Li-CO_2 batteries. Angew. Chem. Int. Ed. *54*, 6550–6553.

19. Lim, H.D., Park, H., Kim, H., Kim, J., Lee, B., Bae, Y., Gwon, H., and Kang, K. (2015). A new perspective on Li-SO_2 batteries for rechargeable systems. Angew. Chem. Int. Ed. *54*, 9663–9667.

20. Al Sadat, W.I., and Archer, L.A. (2016). The O_2-assisted Al/CO_2 electrochemical cell: A system for CO_2 capture/conversion and electric power generation. Sci. Adv. *2*, e1600968.

21. Hu, X., Li, Z., Zhao, Y., Sun, J., Zhao, Q., Wang, J., Tao, Z., and Chen, J. (2017). Quasi-solid state rechargeable Na-CO_2 batteries with reduced graphene oxide Na anodes. Sci. Adv. *3*, e1602396.

22. Liu, Y.L., Wang, R., Lyu, Y.C., Li, H., and Chen, L.Q. (2014). Rechargeable Li/CO_2-O_2 (2:1) battery and Li/CO_2 battery. Energy Environ. Sci. *7*, 677–681.

23. Jung, H.G., Hassoun, J., Park, J.B., Sun, Y.K., and Scrosati, B. (2012). An improved high-performance lithium-air battery. Nat. Chem. *4*, 579–585.

24. Ohzuku, T., Iwakoshi, Y., and Sawai, K. (1993). Formation of lithium-graphite intercalation compounds in nonaqueous electrolytes and their application as a negative electrode for a lithium ion (shuttlecock) cell. J. Electrochem. Soc. *140*, 2490–2498.

25. Zhu, D., Zhang, L., Ruther, R.E., and Hamers, R.J. (2013). Photo-illuminated diamond as a solid-state source of solvated electrons in water for nitrogen reduction. Nat. Mater. *12*, 836–841.

26. Sun, Y., Li, Y., Sun, J., Li, Y., Pei, A., and Cui, Y. (2017). Stabilized Li_3N for efficient battery cathode prelithiation. Energy Storage Materials *6*, 119–124.

27. Park, K., Yu, B.C., and Goodenough, J.B. (2015). Li_3N as a cathode additive for high-energy-density lithium-ion batteries. Adv. Energy Mater. *6*, 1502534.

28. Aurbach, D., Youngman, O., Gofer, Y., and Meitav, A. (1990). The electrochemical behavior of 1,3-dioxolane-$LiClO_4$ solutions-I. Uncontaminated solutions. Electrochim. Acta *35*, 625–638.

29. Aurbach, D., Youngman, O., and Dan, P. (1990). The electrochemical behavior of 1,3-dioxolane-$LiClO_4$ solutions-II. Contaminated solutions. Electrochim. Acta *35*, 639–655.

30. Tsuneto, A., Kudo, A., and Sakata, T. (1994). Lithium-mediated electrochemical reduction of high pressure N_2 to NH_3. J. Electroanal. Chem. *367*, 183–188.

31. Liu, J., Kelley, M.S., Wu, W., Banerjee, A., Douvalis, A.P., Wu, J., Zhang, Y., Schatz, G.C., and Kanatzidis, M.G. (2016). Nitrogenase-mimic iron-containing chalcogels for photochemical reduction of dinitrogen to ammonia. Proc. Natl. Acad. Sci. USA *113*, 5530–5535.

32. Kaiser-Bischoff, I., Boysen, H., Scherf, C., and Hansen, T. (2005). Anion diffusion in Y- and N-doped ZrO_2. Phys. Chem. Chem. Phys. *7*, 2061–2067.

33. Oshikiri, T., Ueno, K., and Misawa, H. (2014). Plasmon-induced ammonia synthesis through nitrogen photofixation with visible light irradiation. Angew. Chem. Int. Ed. *53*, 9802–9805.